A CONDITIONAL EQUITY RISK MODEL FOR REGULATORY ASSESSMENT

BY

A. FLORYSZCZAK, J. LÉVY VÉHEL AND M. MAJRI

ABSTRACT

We define and study in this work a simple model designed for managing long-term market risk of financial institutions with long-term commitments. It allows the assessment of solvency capital requirements and the allocation of risk budgets. This model allows one to avoid over-assessment of solvency capital requirements specifically after market disruptions. It relies on a dampener component in charge of refining risk assessment after market failures. Rather than aiming at a realistic and thus complex description of equity prices movements, this model concentrates on minimal features enabling accurate computation of capital requirements. It is defined both in a discrete and continuous fashion. In the latter case, we prove the existence, uniqueness and stability of the solution of the stochastic functional differential equation that specifies the model. One difficulty is that the proposed underlying stochastic process has neither stationary nor independent increments. We are however able to perform statistical analyses in view of its validation. Numerical experiments show that our model outperforms more elaborate ones of common use as far as medium-term (between 6 months and 5 years) risk assessment is concerned.

KEYWORDS

Risk budget allocation, solvency capital requirement, value-at-risk, procyclicality, stochastic functional differential equation, non-stationary process, market risk allocation.

1. INTRODUCTION AND BACKGROUND

Insurance companies or pension funds with long-term commitments should manage their market risk in a long-term perspective and need to rely on mathematical key indicators to optimize their portfolio's risk/return profile. One of them is the market risk solvency capital. This metric reflects the level of own

Astin Bulletin 49(1), 217-242. doi:10.1017/asb.2018.35

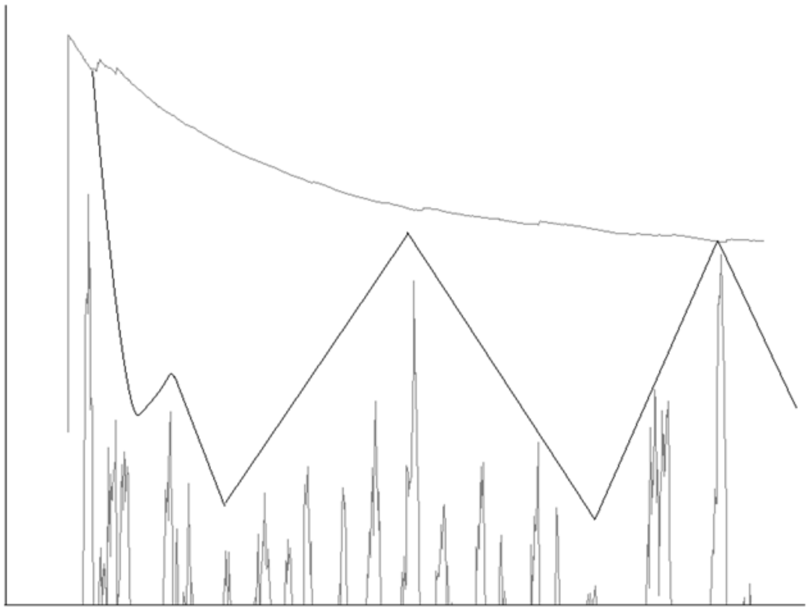

FIGURE 1: S&P 500 losses between December 1927 and December 2014 (irregular curve), 99.5% VaR for geometric Brownian motion (top curve) and for a hypothetical model that would minimize required own funds while remaining prudent (broken lines).

funds or guarantees needed to face the market risk of the managed portfolio. It is used to carry out dynamic asset allocation changes so as to maintain an acceptable level of risk for the company.

The model proposed has the particularity of avoiding excessive over-assessments of solvency capital requirements specifically after market disruption as illustrated in Figure 1. This figure displays the S&P 500 losses between December 1927 and December 2014 (irregular curve), along with the 99.5% VaR for geometric Brownian motion (top curve). As one can see, required own funds are severely overestimated after market downs. An ideal model would minimize required own funds while remaining prudent, as exemplified by the black curve. Of course, such a model seems beyond reach, but one can try to find mechanisms allowing financial companies with long-term commitments to reduce their Solvency Capital Requirement (SCR) in market downs so as to maintain a more stable asset allocation.

This work defines and studies a simple equity risk model with this specific aim. It focuses on risk assessment for a time horizon in the approximate range of 6 months to 5 years. The lower bound makes it possible to avoid a fine modelling of volatility (as, e.g., in stochastic volatility models): indeed, accounting for volatility variations is crucial for short-term horizons, but less so for medium-term ones. The upper bound allows us to ignore complex long-term risk modelling issues. Numerical experiments show that the proposed

https://doi.org/10.1017/asb.2018.35 Published online by Cambridge University Press

model is indeed not suitable for equity derivatives pricing nor for equity risk assessment for horizon terms below 6 months or above 5 years.

Our model exhibits the following desirable features:

- It is simple both conceptually and as far as implementation is concerned.
- Experiments show that its returns are stochastically dominated to the first order by the ones of actual returns for a range of composite indices: as a consequence, risks are not underestimated, a crucial requirement for prudential purposes.
- Thanks to a careful evaluation of VaR during market downs, it mitigates the pro-cyclicality entailed by the market-consistency-based regulation framework, avoiding in particular equities sell-off after disruptions.

Let us elaborate on the last item, which is the core of our approach. Beyond the simple experiment of Figure 1, it is a well-documented fact that implementing solvency capital requirement based on classical models such as geometric Brownian motion may lead to pro-cyclical effects and thus have potentially damageable impacts on the economy (Kashyap and Stein, 2004; Adrian and Shin, 2007; Plantin *et al.*, 2008; Rochet, 2008). This is mainly due to the fact that, in order to fulfil their SCR, insurance and reinsurance companies may have to sell assets during market falls, possibly leading to a vicious circle.

There are two main paths to reduce these effects in the frame of Solvency II. The first one is based on using simple pro-cyclical models but to “correct” them, as far as SCR is concerned, with an a posteriori adjustment of VaR. The regulator has, for example, put forward a “standard formula” for VaR that uses a so-called *dampener* mechanism. Several implementations of dampener have been proposed by the EIOPA (formerly CEIOPS), first in the QIS4 technical specifications, and then, among others, see CEIOPS (2010). The position paper (Solvency Assessment and Management, 2012) offers a unified view of the main variants of the dampener mechanism.

The second path is more elaborate and consists in the introduction of a kind of dampener mechanism within the risk model. In doing so, no a posteriori adjustment of the VaR is needed: instead of post-processing VaRs obtained with geometric Brownian motion or other classical models, this alternative approach designs elaborate models that reflect more closely the nature of equities markets, and in particular those of their features that account for cycles, in the hope that this will lead to counter-cyclical SCR. This is the path taken, for instance, in Bec and Gollier (2009a,b), where a vector autoregressive joint modelling of stocks excess returns and of a certain financial market cycle indicator is proposed. Other models, such as certain stochastic volatility ones that account for empirical properties of volatility such as clustering, long-term dependence or correlation with returns may also be used for more adequate estimations of SCR. A drawback of such models is their complexity, which results in calibration issues: identifying their parameters, specially on short logs, is a difficult task. The impact of any inaccuracy at this stage on the estimation of SCR is hard to assess.

Our work takes a middle term between these two paths: we design a model that is easy to calibrate but at the same time is sufficiently fine so as to mitigate pro-cyclical effects. In a nutshell, the idea is to incorporate the VaR correction of the standard formula as a "continuous time" dampener rather than as an end-of-term one as proposed by the regulator. In a sense that will become clear in the next section, this amounts to avoiding a fine modelling of volatility, as is present in elaborate models and which is responsible for calibration issues, in recognition of the fact that it is more important, in a medium-term time horizon, to model precisely drift than volatility for a correct assessment of equity risk. This view is supported by numerical experiments performed in this article and confirms some observations of, for example, Bec and Gollier (2009a,b).

It is important to realize that our model has no ambition to reflect adequately equity prices returns. Our sole aim is to compute precise mid-term horizon VaRs, a task that does not require reproducing fine properties of the evolution of equity prices, which, as emphasized above, typically leads to calibration issues. Numerical results confirm the relevance of this view. They show, in particular, that our model both meets prudential requirements and mitigates pro-cyclical effects without resorting to an a posteriori adjustment of the VaRs.

This remaining of this article is organized as follows: Section 2 recalls the heuristic construction of our model in a discrete setting, which was introduced in Majri and de Lauzon (2013). A continuous version is studied in Section 3. It is obtained as the unique solution of a stochastic functional differential equation (SFDE): indeed, future increments depend in a non-linear way on a whole range of past values, thus making the use of SFDE mandatory. Section 4 deals with statistical aspects. In particular, we design a specific goodness-of-fit test for the model, whose increments are correlated and non-stationary, and validate it on logs of three indices. Finally, numerical experiments are provided in Section 5. They indicate that our model compares favourably with classical ones such as geometric Brownian motion, GARCH or AR as far as VaR is concerned. More precisely, we consider a proxy for the amount of required own funds and show that, with comparable prudential behaviours, our model always requires less own funds than others, thanks essentially to a better evaluation of VaR in market downs.

2. Heuristic construction

Let us briefly recall the discrete model introduced in Majri and de Lauzon (2013). We let C_i, R_i denote the price and arithmetic return at time i (while the principle of the model is scale free, in practice we work with monthly data). Thus

$$R_{i+1} = \frac{C_{i+1} - C_i}{C_i}.$$

Define S_i as

$$S_i = 2\text{MA}_i(84) - \text{MA}_i(36),$$

where $\text{MA}_i(T)$ is the moving average of C_i computed at time i over the $T+1$ last time instants (months in our case). The model gives the return at time $i+1$ as a function of C_i and S_i:

$$R_{i+1} = \exp(Z_i) - 1 + \frac{1}{12}\left(1 - \frac{C_i}{S_i}\right)^+, \tag{2.1}$$

where $X^+ = \max(0, X)$ and Z_i is a centred Gaussian random variable with variance σ.

Note that we use the same symbols for actual values when they are observed at time i and computed ones at time $i+1$. This should not lead to any confusion in the sequel as it will always be clear from the context which quantity is involved.

The rationale behind this formula is the following one: the added term $\frac{1}{12}(1 - \frac{C_i}{S_i})^+$ is what differentiates the model from pure gBm. It may be understood as a kind of asymmetric implementation of the dampener mechanisms proposed by the regulation authorities. It will increase the return in periods where the price C is smaller than a certain average S of past prices by an amount proportional to the relative excess of S over C. This will reduce the pro-cyclical effect of VaR-based regulation by substituting to the "true" (in the sense of the gBm model) return an "apparent" and larger one when markets are down (i.e., in the lower part of the cycle). This will translate in an "apparent" VaR that is smaller than the "true" one (again in the sense of the gBm model), thus lessening the capital requirement put on financial institutions during stressed periods. In this way, the damaging impact of market downs on SCR is tempered, in agreement with the fact that usually market risk falls after a market shock. However, no adjustment is made when the price is higher than the average, hence the asymmetry. The justification of this asymmetry is empirical: numerical experiments show that it yields better result than a symmetric formula does. The exact form chosen from S does not either have an easy theoretical justification and is rather the result of numerous experiments. However, a heuristic explanation for the use of two moving averages is that it delays the mean reverting effect as compared to the use of only one moving average, thus decreasing the risk of underestimating losses. This analysis is supported by experiments.

Let us now comment on what distinguishes model (2.1) from the dampener proposed by the regulator. The essence of our idea consists in noting that the corrected VaRs given by the dampener mechanisms can in effect be seen as plain VaRs corresponding to a modified model. Our approach then simply consists in enhancing this modified model. Let us explain this in more detail. Since our aim here is to emphasize the benefits of identifying the modified model describing the evolution of returns as opposed to *ex-post* correction of VaR, we consider simplified versions, thus avoiding obscuring the main arguments by technical details. We consider monthly returns and a one-year time horizon, and we compare the QIS5 implementation of dampener, which reads:

$$\mathrm{VaR_D} = \mathrm{VaR} + \frac{C_{i+12} - \mathrm{MA}_{i+12}(36)}{\mathrm{MA}_{i+12}(36)}, \tag{2.2}$$

where $\mathrm{VaR_D}$ is the dampened VaR and VaR is the VaR given by gBm, to the formula

$$R_{i+j} = Z_{i+j-1} + \frac{C_{i+j-1} - \mathrm{MA}_{i+j-1}(36)}{\mathrm{MA}_{i+j-1}(36)} \tag{2.3}$$

for $j = 1, \dots, 12$, which we introduce as a simplified version of (2.1). By construction, (2.2) amounts to replacing the centred Gaussian variable describing the one-year return in the original gBm model by an "apparent" model where the return follows a Gaussian law with same variance but mean equal to $\frac{C_{i+12}-\mathrm{MA}_{i+12}(36)}{\mathrm{MA}_{i+12}(36)}$ (a quantity which is known at the end of the period). In other words, one simply translates the distribution function of the return, introducing a drift equal to $\frac{C_{i+12}-\mathrm{MA}_{i+12}(36)}{\mathrm{MA}_{i+12}(36)}$. With model (2.3), however, this correction is made at each time step: for every $i + j, j = 1, \dots, 12$, the original gBm model is replaced by an apparent one where the drift is $\frac{C_{i+j-1}-\mathrm{MA}_{i+j-1}(36)}{\mathrm{MA}_{i+j-1}(36)}$. Thus, the dampening adjustments are made "continuously" all along the path (or rather, they will be made so in the continuous version developed in the next section) instead of just once at the end of the period. To put it differently, at time $i + 12$, the net correction in model (2.3) depends on the whole path since time i, while the EIOPA dampener depends only on the final price and the moving average of the prices in the considered period. In general, procedures that depend on the whole path are more precise than ones depending only on an average, unless the considered process possesses some "nice" properties such as being strongly Markovian. This fact is the core reason why our model behaves in a more robust way than (2.2). Note that, to achieve such a "continuous" dampening effect, it is essential to incorporate the correction in the evolution of returns as in (2.1) or (2.3). This path-dependent adjustment cannot be implemented using a correction of the sole *ex-post* VaR as in (2.2).

Let us stress again that (2.1) is nothing more than an enhanced version of the implicit model corresponding to the dampener correction of VaR. It is thus by no means a realistic model for the evolution of prices, and this is so for many reasons. For one, it is a rather simple model, with only one free parameter, σ, which does not even depend on time. It is a well-known fact that volatility does vary in time and exhibit important features such as volatility clustering. This is why a host of local and stochastic volatility models have been developed in the past years. As noted in the introduction, however, a fine modelling of volatility is less important for one-year returns than for short period ones. A second aspect is that the model does not allow for jumps and will thus lead to tails for returns which will not display the fat tails that are commonly encountered on markets. Finally, it should be noted that the added term $\frac{1}{12}(1 - \frac{C_i}{S_i})^+$ is always non-negative and is positive with positive probability. As a consequence, the evolution predicted by (2.1) will lead to prices which are, in the long term, significantly larger than the ones given by gBm for the same set of parameters.

Although this model is not an adequate representation of reality, it appears that it allows one to evaluate one-year VaRs in an accurate but simple way that greatly reduces pro-cyclical effects. While this fact cannot be easily proved in a theoretical fashion, it is supported by exhaustive numerical experiments, some of which are presented in Section 5. Heuristically, this is also justified by the same arguments as the ones put forward by the regulators when introducing the various dampener mechanisms.

From a numerical point of view, computing VaRs with our model is more complex than with the dampener proposed by the regulator: indeed, a closed formula for VaR is not available any more, and one has to resort to Monte-Carlo simulations. The added computational burden is however small, and VaRs can be obtained in a simple and quick way.

The model will be defined more generally in the next section and its parameters will be calibrated in Section 5. Note that the idea of lifting the VaR correction into the evolution equation can be implemented with models other than gBm. As an example, we have explored the case of a Variance-Gamma model (see Section 5.2). Yet other variants could be considered.

3. The model

Even though we do not claim that the discrete equation presented in the previous section is a realistic model for the evolution of prices, it is still important to check that it leads to a well-defined stochastic process when the time step tends to 0. This will allow us in particular to be confident that the VaRs it will yield are meaningful at all time scales. Having available a continuous time version also makes it easier to study the dependency on the various parameters, and in particular to assess stability.

We thus study in this section a continuous version of Model (2.1). We will use the following notations. The moving average of the price C over the time period $[t - T, t]$ is denoted $A_{t,T}$:

$$A_{t,T} = \frac{1}{T} \int_{t-T}^{t} C(u)\, du. \tag{3.1}$$

Set

$$S_t = 2A_{t,T_1} - A_{t,T_2}. \tag{3.2}$$

When time is measured in months, we will typically use $T_1 = 84$, $T_2 = 36$ as in the previous section. In general, we will always assume that $T_1 > T_2$. Define the function

$$F(\overline{C_{t,T_1}}) = \left(1 - \frac{C_t}{S_t}\right)^+, \tag{3.3}$$

where

$$\overline{C_{t,T_1}} = \{C(t-s), 0 \leq s \leq T_1\}. \tag{3.4}$$

The following equation is a continuous version of the discrete model of Majri and de Lauzon (2013):

$$dC_t = \left(F(\overline{C_{t,T_1}}) + \mu + \frac{\sigma^2}{2}\right) C_t\, dt + \sigma\, C_t dB_t. \tag{3.5}$$

which, by Itô's Formula, is the same as:

$$d(\ln{(C_t)}) = (F(\overline{C_{t,T_1}}) + \mu)\, dt + \sigma\, dB_t. \tag{3.6}$$

Equation (3.5) is not a standard stochastic differential equation, as F depends on past values of C and not only on C_t. Rather, it belongs to the class of so-called *stochastic functional differential equations* (SFDE). Among the many results about such equations, the one that we will use is as follows (Mao, 1997, Theorem 2.2, p. 150).

Denote E the set of continuous functions from $[-T_1, 0]$ to $\mathbb{R}$, equipped with the norm $||\varphi|| = \sup_{-T_1 \leq u \leq 0} |\varphi(u)|$. Thus, for instance, F defined in (3.3) is a function from E to $\mathbb{R}$. It is useful to regard $\overline{C_{t,T_1}}$ as an E-valued stochastic process.

For a function G from E to $\mathbb{R}$, one considers the following SFDE:

$$dC(t) = G(\overline{C_{t,T_1}})dt + \sigma\, C_t dB(t), \tag{3.7}$$

with initial condition

$$\overline{C_{0,T_1}} = \xi := \{\xi(s), -T_1 \leq s \leq 0\}, \tag{3.8}$$

where ξ is assumed to be $\mathcal{F}_0$-measurable.

By definition, $C(t)$ is called a solution of (3.7) on $[-T_1, T]$, $T > 0$, with initial condition (3.8) if

- $C(t)$ is continuous and, for all $t \in [0, T]$, $\overline{C_{t,T_1}}$ is $\mathcal{F}_t$-adapted;
- $G(\overline{C_{t,T_1}})$ is integrable on $[0, T]$;

https://doi.org/10.1017/asb.2018.35 Published online by Cambridge University Press

- $\overline{C_{0,T_1}} = \xi$ and, for all $t \in [0, T]$,

$$C(t) = \xi(0) + \int_0^t G(\overline{C_{s,T_1}})ds + \sigma \int_0^t C_s dB(s)$$

almost surely.

The solution is said to be unique if, for any other solution C',

$$\mathbb{P}\left(C(t) = C'(t)\ \forall t \in [-T_1, T]\right) = 1,$$

that is, C and C' are indistinguishable.

Theorem 1. *[Mao (1997, Theorem 2.2, p. 150)] Assume that there exists $K > 0$ such that, for all φ, ψ in E:*

1. $|G(\varphi) - G(\psi)| \leq K||\varphi - \psi||$,
2. $G(\varphi)^2 \leq K(1 + ||\varphi||)^2$.

Then there exists a unique solution C to (3.7) with initial condition (3.8). Furthermore, this solution verifies $\mathbb{E}\left(\int_{-T_1}^{T} C(t)^2 dt\right) < \infty$.

Our model (3.5) is of the form (3.7) with $G(\overline{C_{t,T_1}}) = (F(\overline{C_{t,T_1}}) + \frac{\sigma^2}{2})C_t$. Unfortunately, Theorem 1 does not apply in our situation. Indeed, it is easy to see that, since S ranges in $\mathbb{R}$, G cannot fulfil its assumptions.

However, empirical evidence shows that S_t almost always remains positive and bounded away from 0 on all analysed assets. Furthermore, in the rare situations where S_t comes close to 0 or gets negative, the philosophy of the model would be to set $F = 0$.

These considerations prompt us to modify (3.3) as follows:

$$F_1(\overline{C_{t,T_1}}) = \left(1 - \frac{C_t}{S_t}\right)^+ \mathbb{1}(S_t > \varepsilon),$$

where ε is positive real number which may be chosen as small as desired.

While these modifications prevent explosion of G, they introduce a discontinuity at the value ε, which again forbids the use of Theorem 1. To avoid this, we introduce yet another variant as follows:

$$F_2(\overline{C_{t,T_1}}) = \frac{(S_t - C_t)^+}{S_t}\mathbb{1}(S_t > \varepsilon) + S_t\frac{(\varepsilon - C_t)^+}{\varepsilon^2}\mathbb{1}(0 \leq S_t \leq \varepsilon) \tag{3.9}$$

3.1. Existence and uniqueness

Proposition 1. *Let*

$$G(\overline{C_{t,T_1}}) = \left(\frac{(S_t - C_t)^+}{S_t}\mathbb{1}(S_t > \varepsilon) + S_t\frac{(\varepsilon - C_t)^+}{\varepsilon^2}\mathbb{1}(0 \leq S_t \leq \varepsilon) + \frac{\sigma^2}{2}\right) C_t.$$

https://doi.org/10.1017/asb.2018.35 Published online by Cambridge University Press

Then G satisfies Assumptions 1 *and* 2 *of Theorem* 1*. As a consequence, for any* $T > 0$*, the equation*

$$dC_t = \left(F_2(\overline{C_{t,T_1}}) + \frac{\sigma^2}{2} \right) C_t \, dt + \sigma C_t dB_t \tag{3.10}$$

with initial condition (3.8) *has a unique solution* C *on* $[-T_1, T]$*. Furthermore,* $\mathbb{E}\left(\int_{-T_1}^{T} C(t)^2 dt \right) < \infty$.

Proof. Assumption *1* says that G must be a Lipschtz function of its argument, which is a continuous function from $[-T_1, 0]$ to $\mathbb{R}$. Remark that:

- A, as defined in (3.1), is a Lipschtz function of $\overline{C_{t,T_1}}$.
- By (3.2), the same is true of S_t.
- The right-hand side of (3.9) defines a function that is Lipschtz both in S_t and C_t.

By composition, F_2 is itself a Lipschtz function of $\overline{C_{0,T_1}}$, and Assumption *1* is satisfied.

Assumption *2* is obviously verified since F_2 ranges in [0, 1].

Theorem 1 then ensures existence and uniqueness of the solution of (3.10). ■

3.2. Stability

It is a well-known fact that solutions of standard SDEs are stable with respect to small modifications of the model. That is, if the functions defining the SDE undergo a small variation (in a certain sense), then the solution is also only slightly modified. See, for instance, Friedman (1975, Theorem 5.2 p.118) or Protter (2004, Theorem 9 p. 257) for precise statements. This is important in practice since, for the model to be trustworthy, one needs to check that if the parameters (which, in our case are T_1, T_2, σ and ε) are estimated in a slightly inaccurate way, then the output remains roughly the same, and so do the VaRs computed based on it.

Although we believe a general result for SFDE should exist, we have not been able to spot one. For this reason, we prove stability in our particular case.

Proposition 2. *Let* $(T_1^{(n)}, T_2^{(n)}, \sigma^{(n)})_n$ *be a sequence of strictly positive elements of* $\mathbb{R}^3$*, with* $T_1^{(n)} > T_2^{(n)}$ *for all n, converging to* (T_1, T_2, σ) *where* $T_1 > T_2 > 0, \sigma > 0$*. Fix* $\varepsilon > 0$*. Consider, for* $n \in \mathbb{N}$*, the SFDE:*

$$dC_t^{(n)} = G^{(n)} \left(\overline{C_{t,T_1^{(n)}}^{(n)}} \right) dt + \sigma^{(n)} C_t^{(n)} dB_t, \tag{3.11}$$

https://doi.org/10.1017/asb.2018.35 Published online by Cambridge University Press

with initial condition (3.8)*, where*

$$G^{(n)}\left(\overline{C^{(n)}_{t,T_1^{(n)}}}\right)=\left(\frac{(S_t^{(n)}-C_t^{(n)})^+}{S_t^{(n)}}\mathbb{1}(S_t^{(n)}>\varepsilon)\right.$$
$$\left.+S_t^{(n)}\frac{(\varepsilon^{(n)}-C_t^{(n)})^+}{(\varepsilon)^2}\mathbb{1}(0\leq S_t^{(n)}\leq\varepsilon)+\frac{(\sigma^{(n)})^2}{2}\right)C_t^{(n)}$$

and

$$S_t^{(n)}=2\frac{1}{T_1^{(n)}}\int_{t-T_1^{(n)}}^{t}C^{(n)}(u)\,du-\frac{1}{T_2^{(n)}}\int_{t-T_2^{(n)}}^{t}C^{(n)}(u)\,du.$$

Then, as n tends to infinity, the unique solution $C^{(n)}$ *to* (3.11) *converges to the one of* (3.10) *in the following sense:*

$$\lim_{n\to\infty}\mathbb{E}\left(\sup_{0\leq t\leq T}|C^{(n)}(t)-C(t)|^2\right)=0. \tag{3.12}$$

Proof. The proof draws, on the one hand, on the proof of existence and uniqueness for the solution of an SFDE and, on the other hand, on the classical proof of stability for standard SDEs.

The fact that Equation (3.11) has a unique solution for each n is proved in the same way as Proposition 1.

Write, for $0\leq u\leq t\leq T$,

$$C_u^{(n)}-C_u=\eta_n(u)+\int_0^u\left(G^{(n)}\left(\overline{C^{(n)}_{s,T_1^{(n)}}}\right)-G^{(n)}(\overline{C_{s,T_1}})\right)\,ds+\sigma^{(n)}\int_0^u\left(C_s^{(n)}-C_s\right)dB_s,$$

where

$$\eta_n(u)=\int_0^u\left(G^{(n)}(\overline{C_{s,T_1}})-G(\overline{C_{s,T_1}})\right)\,ds+\left(\sigma^{(n)}-\sigma\right)\int_0^u C_s\,dB_s.$$

Then

$$(C_u^{(n)}-C_u)^2\leq 3\,\eta_n(u)^2+3\,\left(\int_0^u\left(G^{(n)}\left(\overline{C^{(n)}_{s,T_1^{(n)}}}\right)-G^{(n)}(\overline{C_{s,T_1}})\right)\,ds\right)^2$$
$$+3\,\left(\sigma^{(n)}\int_0^u\left(C_s^{(n)}-C_s\right)\,dB_s\right)^2.$$

Using the Lipschitz condition on $G^{(n)}$, the convergence of the sequence $(\sigma^{(n)})_n$ and the fact that $C^{(n)}$ and C coincide before time 0, one sees that

$$\mathbb{E}\left(3\,\left(\int_0^u\left(G^{(n)}\left(\overline{C^{(n)}_{s,T_1^{(n)}}}\right)-G^{(n)}(\overline{C_{s,T_1}})\right)\,ds\right)^2+3\,\left(\sigma^{(n)}\int_0^u\left(C_s^{(n)}-C_s\right)\,dB_s\right)^2\right)$$
$$\leq K\int_0^u\mathbb{E}||C_s^{(n)}-C_s||^2\,ds\leq K\int_0^t\mathbb{E}\left(\sup_{0\leq r\leq s}|C_r^{(n)}-C_r|^2\right)\,ds,$$

https://doi.org/10.1017/asb.2018.35 Published online by Cambridge University Press

where K is constant depending only on T (that may change from line to line when used in the sequel). As a consequence,

$$\mathbb{E}\left(\sup_{0\le u\le t}(C_u^{(n)}-C_u)^2\right)\le K\,\mathbb{E}\left(\sup_{0\le u\le t}\eta_n(u)^2\right)+K\int_0^t\mathbb{E}\left(\sup_{0\le r\le s}|C_r^{(n)}-C_r|^2\right)ds. \tag{3.13}$$

Now,

$$\mathbb{E}\left(\sup_{0\le u\le t}\eta_n(u)^2\right)\le K\left(\int_0^t\mathbb{E}\left(G^{(n)}(\overline{C_{s,T_1}})-G(\overline{C_{s,T_1}})\right)^2\,ds\right.$$
$$\left.+\left(\sigma^{(n)}-\sigma\right)^2\int_0^t\mathbb{E}(C_s^2)\,ds\right).$$

Since $\int_0^T\mathbb{E}(C_s^2)\,ds$ is finite, the term $\left(\sigma^{(n)}-\sigma\right)^2\int_0^t\mathbb{E}(C_s^2)\,ds$ tends to 0 when n tends to infinity.

Furthermore, by examining the forms of $G^{(n)}$ and G, one easily checks that, for all positive N,

$$\lim_{n\to\infty}\sup_{\varphi\in E,||\varphi||\le N}|G^{(n)}(\varphi)-G(\varphi)|=0. \tag{3.14}$$

As a consequence, using a classical localization argument, one has that $\mathbb{E}\left(\sup_{0\le u\le t}\eta_n(u)^2\right)$ tends to 0 when n tends to infinity. Inequality (3.13) and the Gronwall lemma allow to conclude that (3.12) indeed holds. ■

Note that the result does not hold anymore if one also allows ε to vary: that is, if one considers a sequence of equations as (3.11) where ε is replaced by a sequence $\varepsilon^{(n)}$ which tends to ε, one cannot guarantee that the sequence of solutions $C^{(n)}$ will converge to C. This is because (3.14) does not hold in the situation. This is however of little consequence in practice.

4. Statistical analysis

We perform in this section a statistical analysis which suggests that our model is able to some extent reproduce prudential aspects of observed returns. In that view, we build a goodness-of-fit test for which we provide empirical justification.

Since our model generates neither stationary nor independent increments, many usual tools in statistics are not available in our case. For this reason, we use an indirect approach and base our tests on (1) Bernoulli random variables detecting the violations of either historical or simulated returns, that is, the occurrences of the event “the return is smaller than the one predicted by the model at confidence level p”, and (2) averages of these random variables. Considering these quantities makes sense in a prudential context, where the main concern is to evaluate VaR.

Let us first recall and fix some notations. We let r_i (resp. $\hat{r}_i$) denote the historical (resp. simulated) return at month i, and R_T (resp. $\widehat{R_T}$) the historical (resp. simulated) annual return between months T and $T+12$. Thus:

$$1 + R_T = \prod_{i=T}^{T+11} (1 + r_i), \; 1 + \widehat{R_T} = \prod_{i=T}^{T+11} (1 + \hat{r}_i). \tag{4.1}$$

We let $F_{\widehat{R}_t}$ (resp. F_{R_t}) denote the cumulative distribution functions (cdf) of $\widehat{R}_t$ (resp. R_t). No closed form exists for $F_{\widehat{R}_t}$, but it may be approximated to any desired accuracy by Monte-Carlo simulation. Let $Q_{t,M}$ be such an approximation obtained with M draws. In the following, p will always denote the confidence level.

4.1. Building blocks

4.1.1. *Definitions and dependence.*
In this section we define the "building blocks" of our test: we consider the Bernoulli random variables defined by $\mathbb{1}(R_T \leq F^{-1}_{\widehat{R_T}}(p))$ and $\mathbb{1}(\widehat{R_T} \leq F^{-1}_{\widehat{R_T}}(p))$. Since $F_{\widehat{R_T}}$ is unknown, we approximate these variables by the following ones:

$$Y^p_T = \mathbb{1}_{R_T \leq Q^{-1}_{T,M}(p)}$$

and

$$\widehat{Y}^p_T = \mathbb{1}_{\widehat{R_T} \leq Q^{-1}_{T,M}(p)}.$$

We have remarked previously that, by increasing M, which is independent of all other variables, the distribution of the Y^p_T (resp. $\widehat{Y}^p_T$) will be as close as desired to the one of the $\mathbb{1}(R_T \leq F^{-1}_{\widehat{R_T}}(p))$ (resp. $\mathbb{1}(\widehat{R_T} \leq F^{-1}_{\widehat{R_T}}(p))$). With an abuse of notation, in the sequel, we will use interchangeably Y^p_T and $\mathbb{1}(R_T \leq F^{-1}_{\widehat{R_T}}(p))$ and the same for $\widehat{Y}^p_T$ and $\mathbb{1}(\widehat{R_T} \leq F^{-1}_{\widehat{R_T}}(p))$.

We wish to test two hypotheses:

$\mathcal{H}_0$: *the random variables* Y^p_T *are iid Bernoulli with parameter* p.

$\widehat{\mathcal{H}}_0$: *the random variables* $\widehat{Y}^p_T$ *are iid Bernoulli with parameter* p.

Under $\mathcal{H}_0$, our model is a prudential one for violations at level p of observed returns. The relevance of $\widehat{\mathcal{H}}_0$ lies in the "independent" assumption: indeed, by definition, each $\widehat{Y}^p_T$ is Bernoulli random variable with parameter p. However, independence is not guaranteed. To the contrary, since there is a strong overlap between successive $\widehat{Y}^p_T$, we do not expect these variables to be independent.

A possibility to test the hypothesis $\mathcal{H}_0$ is to compute the following counting statistics (the case of $\widehat{\mathcal{H}}_0$ is similar): we define two classes, $C_0 = \{i : Y^p_i = 0\}$ and $C_1 = \{i : Y^p_i = 1\}$. Under the null hypothesis, the number of elements N_0 and N_1 observed in classes C_0 and C_1 should be close to the theoretical ones, namely Np and $N(1-p)$, respectively, where we recall that N is the total number of observations and p is the Bernoulli parameter.

We are thus led to consider the statistics

$$S = \frac{(Np - N_0)^2}{Np} + \frac{(N(1-p) - N_1)^2}{(N(1-p))}.$$

We expect S to follow a χ^2 law with one degree of freedom. Experiments show that $\mathcal{H}_0$ and $\widehat{\mathcal{H}}_0$ are rejected.

However, if one considers a sub-sampled sequence $\widehat{Y}_i^p, \widehat{Y}_{k+r}^p, \widehat{Y}_{2k+r}^p, \ldots$ for a sufficiently large k (of the order of 100) and arbitrary but fixed r and performs not only first-order tests but also higher order ones, then $\widehat{\mathcal{H}}_0$ is not rejected. Here, higher order tests means that, for order 2 for instance, we consider the classes

$$C_{00} = \left\{(i,j) : \widehat{Y}_{ik+r}^p = \widehat{Y}_{jk+r}^p = 0\right\},$$
$$C_{01} = \left\{(i,j) : \widehat{Y}_{ik+r}^p + \widehat{Y}_{jk+r}^p = 1\right\},$$
$$C_{11} = \left\{(i,j) : \widehat{Y}_{ik+r}^p = \widehat{Y}_{jk+r}^p = 1\right\},$$

with theoretical sizes, respectively, $p^2N/2$, $2p(1-p)N/2$ and $(1-p)^2N/2$.[1] Denoting observed sizes by N_{00}, N_{01} and N_{00}, we are now interested in the statistics

$$\frac{(p^2N/2 - N_{00})^2}{p^2N/2} + \frac{(2p(1-p)N/2 - N_{01})^2}{2p(1-p)N/2} + \frac{((1-p)^2N/2 - N_{11})^2}{(1-p)^2N/2},$$

which is supposed to follow a χ^2 law with two degrees of freedom.

It thus seems plausible that sufficiently far apart random variables $\widehat{Y}_T^p$ are not correlated, a property that we explore more precisely in the next section.

4.1.2. *m-dependence and consequences.*

We provide in this section experimental evidence that the sequence $(\widehat{Y_T^p})_T$ is m-dependent for m sufficiently large. Let us first briefly recall the notion of m-dependence. Define a distance between two subsets A, B of $\mathbb{N}$ as follows:

$$d(A, B) = \inf\{|i - j|, i \in A, j \in B\}.$$

A sequence (X_j) of random variables is said to be m-dependent if for all couple (A, B) of subsets of $\mathbb{N}$ such that $d(A, B) > m$, the sets $\{X_i, i \in A\}$ and $\{X_i, i \in B\}$ are independent. As we expect that the correlations between the random variables Y_t^p and $Y_{t'}^p$ disappear when $|t - t'|$ gets large (the previous section hints that $|t - t'| > 100$ is a suitable value), we may try to verify experimentally whether m-dependence holds in our case. In that view, we estimate the autocorrelations of the sequence $\widehat{Y}_t^p$. Note that, since we have no reasons to believe that this sequence is stationary, the autocorrelation between say $\widehat{Y}_t^p$ and $\widehat{Y}_{t+\delta}^p$ may in general differ from the one between say $\widehat{Y}_{t'}^p$ and $\widehat{Y}_{t'+\delta}^p$ for $t \neq t'$. This is why we draw on Figure 2 sample autocorrelations between $\widehat{Y}_t^p$ and $\widehat{Y}_{t+\delta}^p$ for

https://doi.org/10.1017/asb.2018.35 Published online by Cambridge University Press

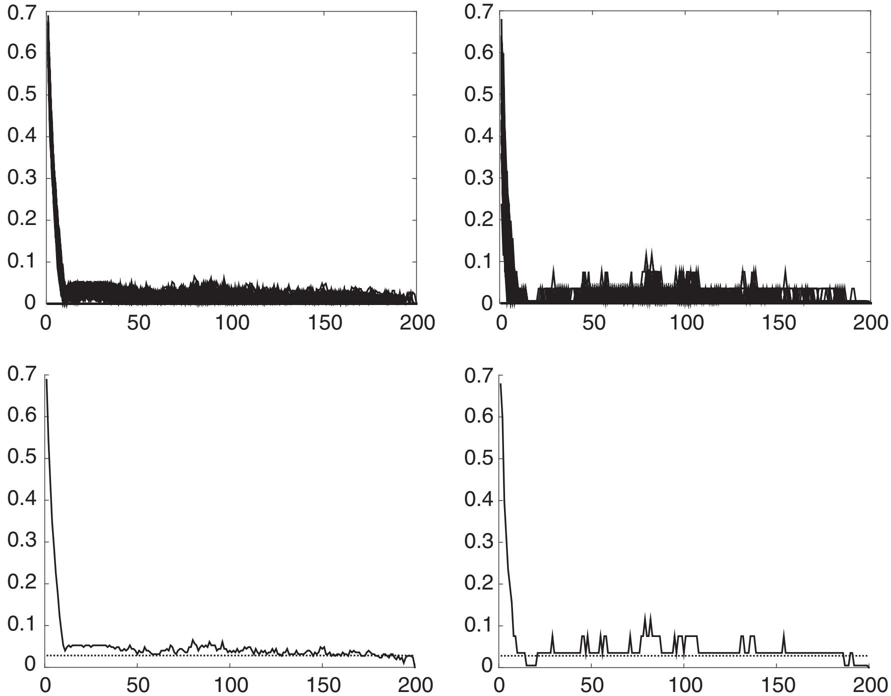

FIGURE 2: Top : autocorrelations between the $\widehat{Y}_t^p$ for various starting times, lags between 0 and 200 and $p = 0.05$ (left) and $p = 0.005$ (right). Bottom: maximum over all starting times of the autocorrelations between the $\widehat{Y}_t^p$ for lags between 0 and 200 and $p = 0.05$ (left) and $p = 0.005$ (right). The horizontal dotted line corresponds to the 95% confidence interval.

$\delta = 0, \ldots, 200$ and a number of starting times t with $p = 0.1$ and $p = 0.05$, along with the maximum over all starting times t of these autocorrelations. As is apparent on the graphs, it seems plausible that the random variables $\widehat{Y}_t^p$ are indeed m-dependent for m of the order of 180 or larger.

A major interest of m-dependence sequences is that they obey, under certain additional conditions, a central limit theorem that we recall now.

Theorem 2. (*Hoeffding and Robbins,* 1948) *Let* $(X_i)_i$ *be a sequence of* m*-dependent random variables such that, for all i,* $\mathbb{E}(X_i) = 0$ *and* $\mathbb{E}\left(|X_i|^3\right) < \infty$. *Set :*

$$A_i = \mathbb{E}\left(X_{i+m}^2\right) + 2\sum_{j=1}^{m} \mathbb{E}\left(X_{i+m-j}X_{i+m}\right).$$

Then, if, for all i,

$$\lim_{p\to\infty} p^{-1} \sum_{k=1}^{p} A_{i+k} =: A \tag{4.2}$$

https://doi.org/10.1017/asb.2018.35 Published online by Cambridge University Press

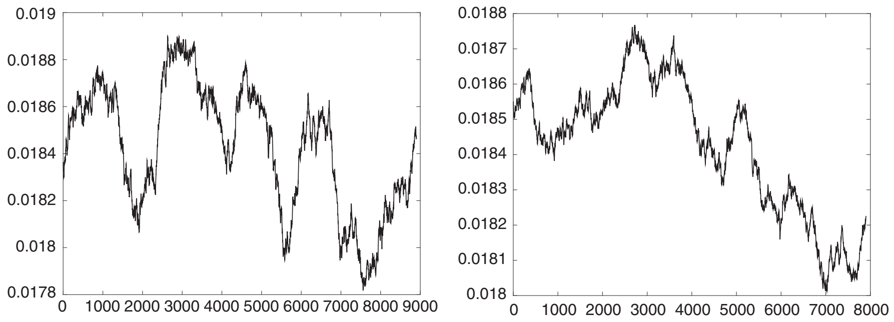

FIGURE 3: Plot of $p^{-1}\sum_{k=1}^{p} A_{i+k}$ for $m = 100$, various starting times i and a confidence level of 99.5%. Left : $p = 1000$. Right : $p = 2000$.

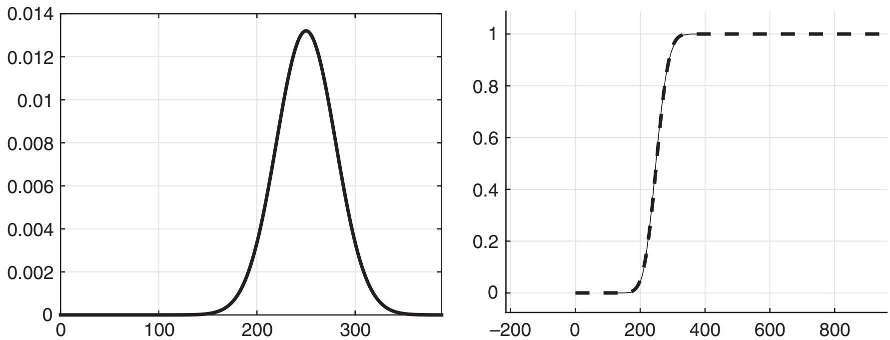

FIGURE 4: Convergence in law of $\widehat{T}_p$ to a normal distribution. Left: empirical pdf for $N = 50,000$ and $p = 0.005$ (10,000 simulations). Right: corresponding (dashed) and theoretical (continuous) cdf.

exists and is independent of i, the random variable $n^{-1/2}(X_1 + \cdots + X_n)$ *tends in law to a centred Gaussian random variable with variance A when n tends to infinity.*

The goodness-of-fit test in the next section will be a direct application of this result. However, in order to use it, we need to verify, at least empirically, that with $X_i = \mathbb{1}\big(\widehat{R}_i \leq F^{-1}_{\widehat{R}_i}(p)\big) - \mathbb{E}\big(\mathbb{1}\big(\widehat{R}_i \leq F^{-1}_{\widehat{R}_i}(p)\big)\big)$, the limit in (4.2) exists and is independent of i. In that view, we compute the renormalized $p^{-1}\sum_{k=1}^{p} A_{i+k}$ for $m = 100$ and various values of i and p and a confidence level of 99.5%. The results are plotted on Figure 3 for two values of p. As one can see, on both graphs (i.e., for $p = 1000$ and $p = 2000$) and for all i, the value is very close to 0.0184. This gives an experimental support to the fact that A does exist independently of i. Furthermore, it is remarkable that its value is equal (within very small statistical fluctuations) to the empirical variance of $n^{-1/2}(X_1 + \cdots + X_n)$ that may be estimated independently to be 0.0187. Note that this empirical verification that the assumptions and results of Theorem 2 hold explains the graphs in Figure 4 as well as the slope in Figure 5.

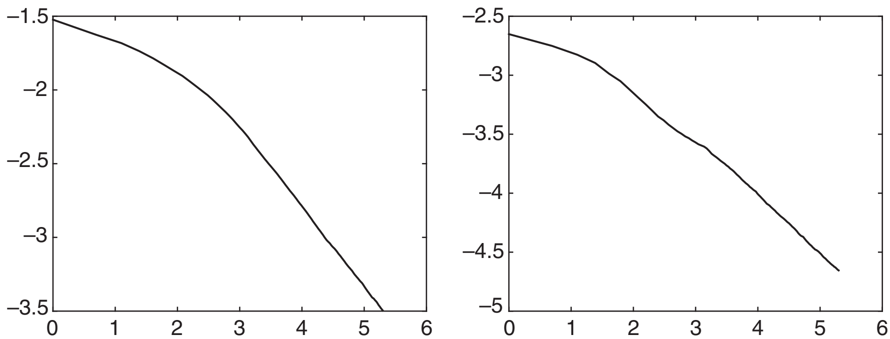

FIGURE 5: Logarithm of the empirical standard deviation of $\widehat{T}_p$ as a function of the logarithm of n for $p = 0.05$ (left) and $p = 0.005$ (right).

4.2. Statistical test

4.2.1. *Definition of the statistics.*
We set up in this section a test based on averages of the Bernoulli random variables considered in the previous section. We introduce the following statistics:

- $T_p = \frac{1}{n}\sum_{t=1}^{n} \mathbb{1}(R_t \leq F^{-1}_{\widehat{R}_t}(p))$, which counts the percentage of violations of historical returns, that is, the percentage of historical returns up to time t that fall below the quantile of confidence at level p of the distribution $\widehat{R}_t$. As mentioned above, we approximate T_p by the computable quantity $\frac{1}{n}\sum_{t=1}^{n} Y_t^p$.
- $\widehat{T}_p = \frac{1}{n}\sum_{t=1}^{n} \mathbb{1}(\widehat{R}_t \leq F^{-1}_{\widehat{R}_t}(p))$, which counts the percentage of violations generated by our model. Again, $\widehat{T}_p$ is approximated by $\frac{1}{n}\sum_{t=1}^{n} \widehat{Y_t^p}$.

4.2.2. *Convergence.*
The results in Section 4.1.2 and Theorem 2 make it plausible that $\widehat{T}_p$ converges to a Gaussian law when n tends to infinity.

The numerical experiments below indicate that this indeed seems to be the case (see Figure 4): $\widehat{T}_p$ appears to tend in law to a normal random variable with mean p and variance σ_p that may be computed empirically and coincide with the theoretical value predicted by Theorem 2. Experiments not displayed in this article show that, as expected, convergence is slower when p is smaller. An additional noteworthy fact (see Figure 5) is that the standard deviation of $\widehat{T}_p$ seems to decrease as a power law of the number of observations n, with slope approximately equal to $-1/2$ for n large enough, again in agreement with the statement of Theorem 2.

4.2.3. *Goodness-of-fit test.*
Our aim is to ensure that risk is assessed in a prudential way. As a consequence, it is natural to test for the following inequality:

$$\widehat{R}_t \leq R_t,$$

in distribution for all t. In other words, we wish to verify that $\widehat{R}_t$ is stochastically dominated at first order by R_t. This is the same as testing whether

$$\mathbb{1}(R_t \leq F^{-1}_{\widehat{R}_t}(p)) \leq \mathbb{1}\big(\widehat{R}_t \leq F^{-1}_{\widehat{R}_t}(p)\big)$$

in distribution for all p and all t. We then choose to formulate our null hypothesis as

$$\mathcal{H}_0(p) : T_p \leq \widehat{T}_p,$$

in distribution for all p and all n, which, heuristically, simply means that, on average, the model generates more violations than observed for historical returns.

As shown empirically above, the statistic $\widehat{T}_p$ tends to a normal distribution $\mathcal{N}(\mu(p), \sigma(p))$ when n tends to infinity. We are thus lead to compute the p-value of our test as:

$$p - \text{value}(p) = \mathbb{P}\left[T_p \leq \mathcal{N}(\mu(p), \sigma(p))\right]$$

for any given confidence level p.

In Section 5.3, we choose a significance level equal to 5% and verify numerically that the hypothesis $\mathcal{H}_0(p)$ of first-order stochastic dominance is not rejected for three indices: MSCI, Eurostoxx50 and S&P500.

5. Numerical experiments

5.1. Empirical verification of the stability with respect to the parameters and calibration issues

As shown in Proposition 2, the model is not too sensitive to small changes in its parameters, namely the standard deviation and the durations of the two moving averages. This is a desirable property since, in practice, it is impossible to calibrate these values exactly. We verify empirically this fact in this section, and also explain how we calibrate σ on market data.

5.1.1. *Variation with respect to the duration of the first moving average.*
We fix here the duration of the second moving average to 36 months, and let the duration of the first moving average take the values 48, 60, 72 and 84 months. Here, as well as in the following sections, the initial data are provided by the Eurostoxx50 index.

https://doi.org/10.1017/asb.2018.35 Published online by Cambridge University Press

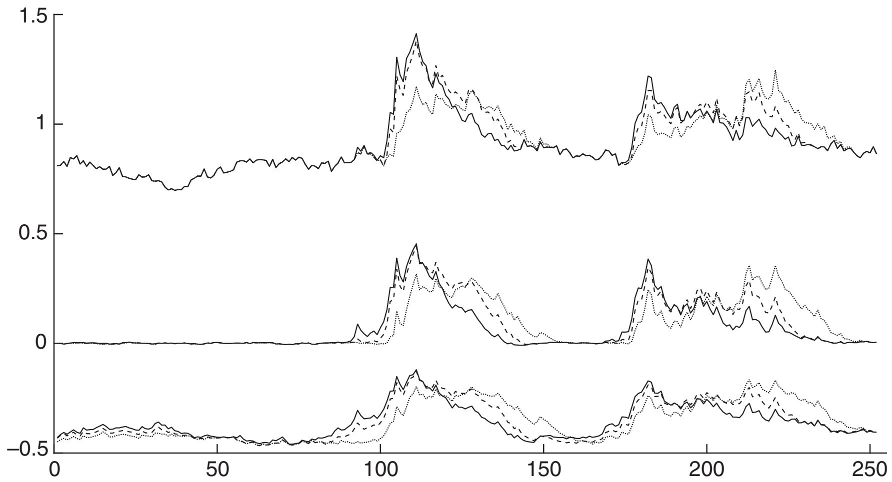

FIGURE 6: Quantiles at levels 0.5%, 50% and 99.5% for the distribution of our model at each date for a fixed duration of 3 years of the second moving average and various durations for the first moving average (4 years: dashed, 5 years: continuous—black—, 7 years: dotted—greyish—).

Figure 6 displays certain quantiles of the distribution of the returns estimated through Monte-Carlo simulations over 240 months. As expected, one can see that the variations with respect to changes in the duration of the first moving average are small.

Extensive tests suggest that a value of 84 months is appropriate for most cases.

5.1.2. *Variation with respect to the duration of the second moving average.*
We now fix the duration of the first moving average 84 months and let the duration of the second one take the values 24, 36, 48 and 60 months.

The results are presented in Figure 7. The same comment as in the previous section can be made. Extensive tests suggest that a value of 36 months is appropriate for most cases.

5.1.3. *Variation and calibration with respect to* σ.
Varying σ translates into a homothetic transformation centred on the middle quantile, as can be seen in Figure 8.

The calibration of σ is asset dependent and is carried out in such a way as to achieve the desired number of violations at a given confidence level p for the duration of the longer moving average. In practice, σ is re-evaluated on a daily basis. While this is a backward looking procedure, the facts that consecutive evaluations seldom differ in a significant way and that the model is stable with respect to σ ensure that this calibration method yields meaningful results. Empirical results show that this procedure typically amounts to multiplying the estimated historical standard deviation by a factor between 1 and 2. As such, it is not unlike the device put forward in the Bale III recommendations that consists in using 3 σ instead of the estimated σ for VaR computations.

https://doi.org/10.1017/asb.2018.35 Published online by Cambridge University Press

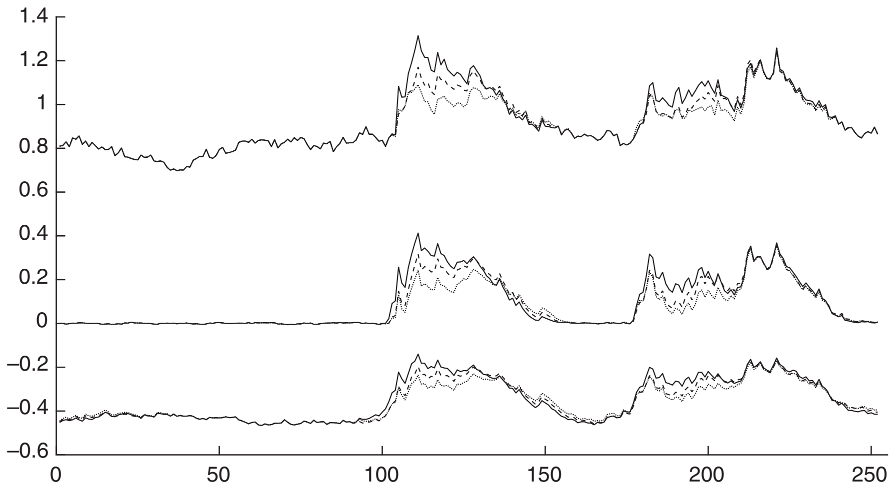

FIGURE 7: Quantiles at levels 0.5%, 50% and 99.5% for the distribution of our model at each date for a fixed duration of 7 years the first moving average and various durations for the second moving average (2 years: dashed, 3 years: continuous—black—, 4 years: dotted—greyish—).

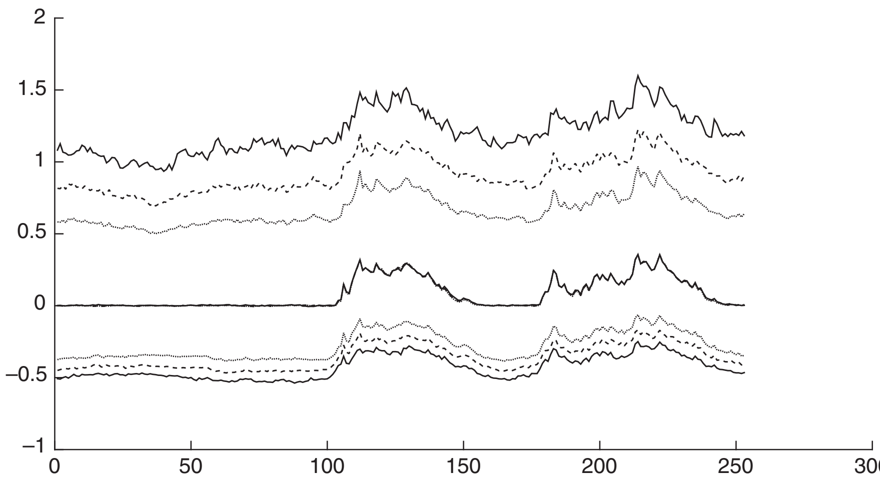

FIGURE 8: Quantiles at levels 0.5%, 50% and 99.5% for the distribution of our model at each date with increasing multipliers for σ : 1 (dotted), 1.3 (continuous -black-) and 1.6 (dashed -greyish-). These numbers refer to the multiplying factor applied to the estimated historical standard deviation.

5.2. Empirical verification of the counter-cyclical property of the model

We present in this section numerical experiments showing that our model yields VaRs which, while being conservative (because of the calibration of σ), does minimize own funds requirements thanks to its counter-cyclical character, as compared with models with similar or greater complexity. Recall that this was our major motivation for introducing our "continuous dampener" mechanism.

To this end, we compare its performances with the one of the three classical models: plain geometric Brownian motion (referred to as "gBm" in the sequel), GARCH(1,1) and AR(1), which are of common use in this context. In order to test whether it would be advantageous to replace the Brownian innovation in (3.5) by a pure jump one, we have also tested our model in the form:

$$dC_t = \left(F(\overline{C_{t,T_1}}) + \mu + \frac{\sigma^2}{2} \right) C_t\, dt + \sigma C_t dV_t, \tag{5.1}$$

where V is a Variance–Gamme process (Madan *et al.*, 1998). This did not result in any significant difference with the Gaussian version, and thus the results obtained with this variant are not shown.

In the sequel, we thus compare four models: gBm, AR(1), GARCH(1,1), and the one described by (3.5), termed BCD (for "Brownian Continuous Dampener").

Let us briefly recall the description of the models AR(1) and GARCH(1,1):

GARCH(1,1)

$$y_t = \sigma_t z_t,$$

$$\sigma_t^2 = \kappa + \gamma \sigma_{t-1}^2 + \alpha y_{t-1}^2,$$

AR(1)

$$y_t = c + \varphi y_{t-1} + \sigma z_t,$$

with y_t the return at time t and z_t Gaussian innovation of mean 0 and variance 1.

For the models AR(1) and GARCH(1,1), the parameters are estimated using the maximum likelihood estimation. We observe that the BCD is fitted on the same number of parameters than AR(1) and GARCH(1,1) models. In other words, with the exception of gBm, which serves as a "baseline", all three other models have exactly three parameters.

To allow for fair comparisons, all models are tested in the same conditions: at each date i, one starts by estimating the parameters using the last 84 monthly data. Then, Monte-Carlo simulations are performed to compute sets of prices for each of the next 12 months, which allows one to obtain VaRs at time $i+12$ months. Since our aim is to compare the models with respect to the amount of SCR they require in a prudential setting, we calibrate the variance as explained in Section 5.1.3: independently for each model, we scale the estimated historical standard deviation in such a way that the proportion of violations is exactly equal to, or slightly smaller than, 0.5%. The exact number of violations for each model is shown in Table 1, along with the associated theoretical value (which depends on the length of each particular log).

Figures 9–14 show graphical comparisons of VaRs obtained at the 99.5% level with the four models along with historical 1-year losses on three indices: monthly MSCI, Eurostoxx50 and S&P500 (for better readability, two graphs

https://doi.org/10.1017/asb.2018.35 Published online by Cambridge University Press

TABLE 1

THEORETICAL AND EMPIRICAL NUMBER OF LOSSES EXCEEDING VAR FOR THE FOUR TESTED MODELS AND THREE TESTED INDICES.

	MSCI	Eurostoxx50	S&P500
Theoretical	2	1	4
gBm	2	1	4
BCD	2	1	4
GARCH(1,1)	1	1	3
AR(1)	2	1	1

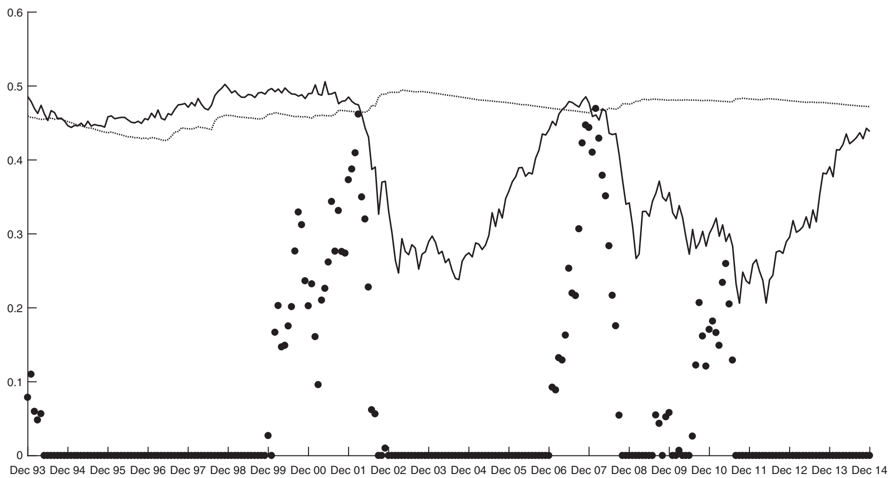

FIGURE 9: Eurostoxx50 monthly data and comparison of historical losses (circles), 99.5% VaRs for the gBm (dotted) and BCD (solid) models.

are displayed for each index: one comparing gBm and BCD, the other GARCH and AR). As is apparent from the figures, our model tends to "dip" after periods of large losses, inducing the sought-after counter-cyclical effect. This is particularly clear when comparing BCD with gBm: they sometimes coincide, as is to be expected, but BCD sharply goes down when appropriate while gBm decreases only slowly. To quantify this fact, we gather on Table 2 the values of an indicator allowing one to assess the quality of the models with respect to their counter-cyclical properties, namely the area under the VaR curve: this serves as a reasonable proxy for the amount of capital required in the model. A good model is one for which this value is "small", provided prudential constraints are met.

As one can see from Tables 1 and 2, with comparable prudential behaviour, our model significantly outperforms gBm, GARCH(1,1) and AR(1) in terms of SCR for the three indices.

We note that, although GARCH(1,1) is, among the four models that we have considered, the one that accounts for the largest number of properties of

TABLE 2

AREAS UNDER VAR FOR THE FOUR TESTED MODELS AND THREE TESTED INDICES.

	MSCI	Eurostoxx50	S&P500
gBm	205	118	436
BCD	185	99	407
GARCH(1,1)	208	117	462
AR(1)	204	118	448

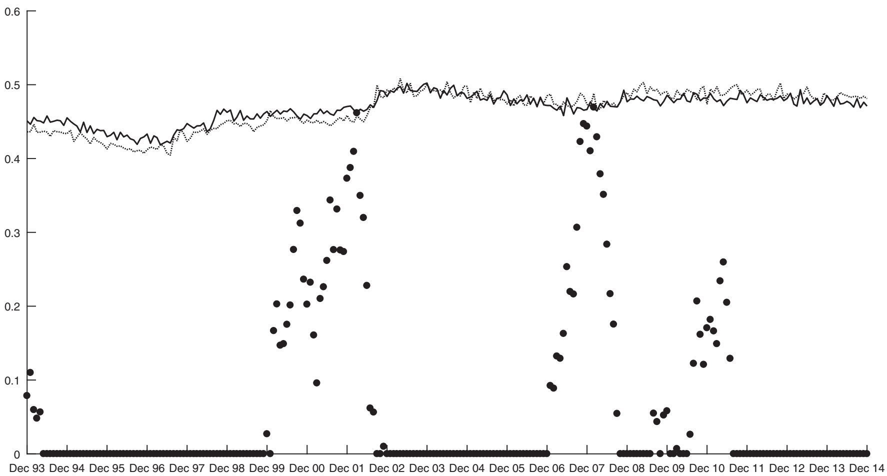

FIGURE 10: Eurostoxx50 monthly data and comparison of historical losses (circles), 99.5% VaRs for the GARCH(1,1) (dotted) and AR(1) (solid) models.

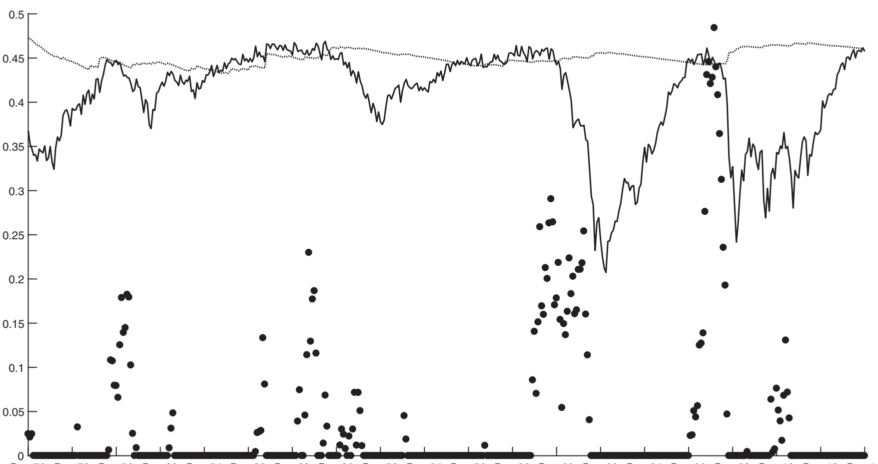

FIGURE 11: MSCI monthly data and comparison of historical losses (circles), 99.5% VaRs for the gBm (dotted) and BCD (solid) models.

https://doi.org/10.1017/asb.2018.35 Published online by Cambridge University Press

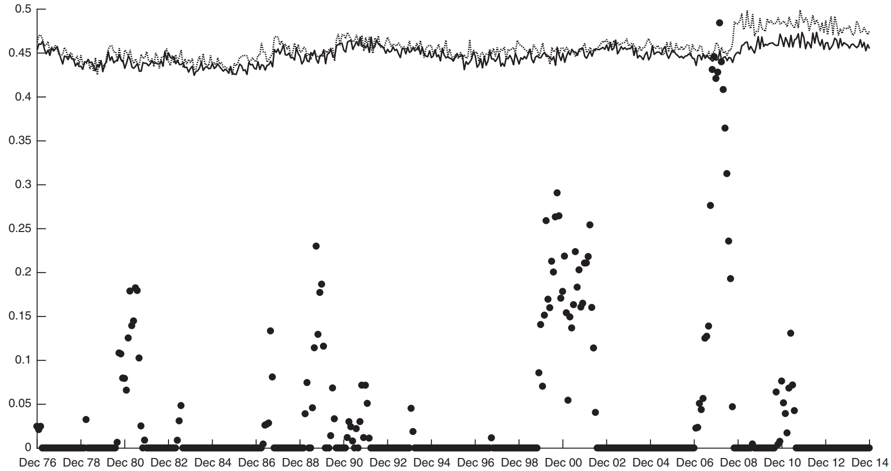

FIGURE 12: MSCI monthly data and comparison of historical losses (circles), 99.5% VaRs for the GARCH(1,1) (dotted) and AR(1) (solid) models.

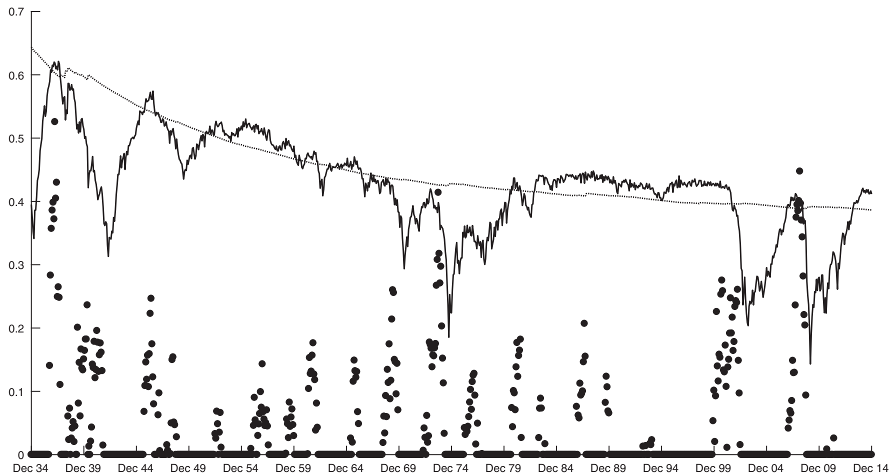

FIGURE 13: S&P500 monthly data and comparison of historical losses (circles), 99.5% VaRs for the gBm (dotted) and BCD (solid) models.

equity returns, it is not the one that yields the most satisfactory results here. This is probably because calibrating the model on short logs as is imposed by our setting is a hard task. As a consequence, the benefit of using a more refined model is counter-balanced by the difficulty of estimating its parameters.

5.3. Empirical verification of the first-order stochastic dominance

As a final validation, we present on Table 3 numerical results for the test setup in Section 4.2.3. We have performed experiments on the three same indices

https://doi.org/10.1017/asb.2018.35 Published online by Cambridge University Press

TABLE 3

p-VALUES FOR OUR MODEL ON THREE INDICES FOR TWO CONFIDENCE LEVELS.

Confidence level	0.5%	5%
MSCI	52.96%	87.48%
Eurostoxx50	53.59%	11.9%
S&P500	56.61%	97.27%

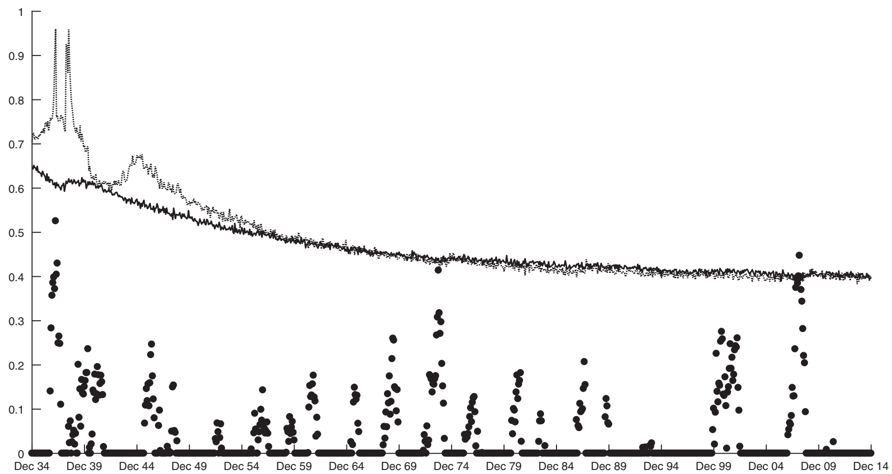

FIGURE 14: S&P500 monthly data and comparison of historical losses (circles), 99.5% VaRs for the GARCH(1,1) (dotted) and AR(1) (solid) models.

as above for two values of the percentile, namely 5% and 0.5%. The model is calibrated with 84 and 36 months for the moving averages and multipliers of historical standard deviation chosen as indicated in the previous section.

For each confidence level, the *p*-values for our model on three indices are widely higher than the significance level of 5% that we defined in Section 4.2.3. Thus hypothesis $\mathcal{H}_0(p)$ of first-order stochastic dominance is not rejected for three indices.

ACKNOWLEDGEMENTS

The authors thank H. Rodarie, P. Desurmont, O. Le Courtois and C. Walter for fruitful discussions on various aspects related to this work, which has been performed in the frame of the SMA research programme.

NOTES

1. For our test to be valid, we need that all couples be independent. This simply amounts to using each index only once. As a consequence, $N/2$ couples (or observations) are available.

https://doi.org/10.1017/asb.2018.35 Published online by Cambridge University Press

References

Adrian, T. and Shin, H.S. (2007) *Liquidity and leverage*, Working Paper, Federal Reserve Bank of New York, New York.

Bec, F. and Gollier, C. (2009a) *Cyclicality and term structure of value-at-risk in Europe*, TSE Working Paper No. 09-035, May 2009.

Bec, F. and Gollier, C. (2009b) *Term structure and cyclicity of value-at-risk: Consequences for the solvency capital requirement*, CESifo Working Paper No. 2596, March 2009.

CEIOPS's Advice for Level 2 Implementing Measures on Solvency II: Article 111 and 304 Equity risk sub-module (2010), https://eiopa.europa.eu/CEIOPS-Archive/Documents/Advices/CEIOPS-L2-Advice-Design-and-calibration-of-the-equity-risk-sub-module.pdf.

Friedman, A. (1975) *Stochastic Differential Equations and Applications*, Vol. 1. New York: Academic Press.

Hoeffding, W. and Robbins, H. (1948) The central limit theorem for dependent random variables, *Duke Mathematical Journal*, **15**(3), 773–780.

Kashyap, A. and Stein, J. (2004) Cyclical implications of the Basel II capital standards. *Federal Reserve Bank of Chicago Economic Perspectives*, **Q1**, 18–31.

Madan, D.P., Carr, E.P. and Chang, E.C. (1998) The variance gamma process and option pricing, *European Finance Review*, **2**, 79–105.

Majri, M. and de Lauzon, F.X. (2013) *An effective equity model allowing long term investments within the framework of Solvency II*, http://hal.archives-ouvertes.fr/docs/00/84/78/87/PDF/MAJRI_20130515.pdf

Mao, X. (1997) *Stochastic Differential Equations and Applications*. Chichester: Horwood Publishing.

Plantin, G., Sapra, H. and Shin, H.S. (2008) Marking-to-market: Panacea or Pandora's box? *Journal of Accounting Research*, **46**, 435–460.

Protter, P.E. (2004) *Stochastic Integration and Differential Equations, Second Edition*. Berlin: Springer-Verlag.

Rochet, J.-C. (2008) *Procyclicality of financial systems: Is there a need to modify current accounting and regulatory rules?* Financial Stability Review, Banque de France, **12**, 95–99.

Solvency Assessment and Management: Steering Committee Position Paper 47 (v 3) Equity risk, https://www.fsb.co.za/Departments/insurance/Documents/PositionPapers/Position%20Paper%2047%20%28v%203%29.pdf.

A. Floryszczak
Groupe SMA
8 rue Louis Armand, CS 71201
75738 Paris Cedex 15, France
E-Mail: anthony_floryszczak@groupe-sma.fr

J. Lévy Véhel (Corresponding author)
Anja team, INRIA & Université de Nantes
2 rue de la Houssiniere, BP 92208
44322 Nantes cedex 3, France
E-Mails: jacques.levy-vehel@inria.fr, jacques.levy.vehel@caselawanalytics.com

M. Majri
Groupe SMA
8 rue Louis Armand, CS 71201
75738 Paris Cedex 15, France
E-Mail: mohamed_majri@groupe-sma.fr

https://doi.org/10.1017/asb.2018.35 Published online by Cambridge University Press